



# Boosting DMFC power output by adding sulfuric acid as a supporting electrolyte: Effect on cell performance equipped with platinum and platinum group metal-free cathodes

Elena Giordano<sup>a</sup>, Enrico Berretti<sup>b</sup>, Laura Capozzoli<sup>b</sup>, Alessandro Lavacchi<sup>b</sup>,  
Mohsin Muhyuddin<sup>c</sup>, Carlo Santoro<sup>c</sup>, Irene Gatto<sup>d</sup>, Andrea Zaffora<sup>e,\*</sup>, Monica Santamaria<sup>e</sup>

<sup>a</sup> Department of Applied Science and Technology, Politecnico di Torino, Corso Duca degli Abruzzi 24, 10129, Torino, Italy

<sup>b</sup> Institute of Chemistry of Organometallic Compounds – National Research Council of Italy (ICCOM-CNR), Via Madonna del Piano 10, 50019, Sesto Fiorentino, Florence, Italy

<sup>c</sup> Electrocatalysis and Bioelectrocatalysis Lab (EBLab), Department of Materials Science, University of Milano-Bicocca, U5, Via Cozzi 5, 20125, Milano, Italy

<sup>d</sup> Institute for Advanced Energy Technologies “Nicola Giordano” (ITAE), Consiglio Nazionale delle Ricerche (CNR), Via Salita S. Lucia sopra Contesse 5, Messina, 98126, Italy

<sup>e</sup> Department of Engineering, University of Palermo, Viale delle Scienze, 90128, Palermo, Italy

## HIGHLIGHTS

- Addition of H<sub>2</sub>SO<sub>4</sub> in methanol feed boosts DMFC power density using Pt/C catalyst.
- Power density is not dependent on H<sub>2</sub>SO<sub>4</sub> concentration using PGM-free catalyst for ORR.
- Addition of H<sub>2</sub>SO<sub>4</sub> does not affect short-term cell performance.
- Catalysts morphology and composition are not affected by H<sub>2</sub>SO<sub>4</sub> presence.

## ARTICLE INFO

### Keywords:

Fuel cells  
Methanol  
Supporting electrolyte  
Electrocatalysis  
Oxygen reduction reaction

## ABSTRACT

Direct methanol fuel cells (DMFCs) are promising electrochemical systems capable of producing electricity from the electrochemical oxidation of methanol and the reduction of oxygen. In this work, the effectiveness of the addition of sulfuric acid as a supporting electrolyte for methanol fuel composition was assessed. The results showed that the peak of power curve in DMFCs with Pt/C cathode electrocatalysts increased progressively from 70 mW cm<sup>-2</sup> (0 mM of H<sub>2</sub>SO<sub>4</sub>) to 115 mW cm<sup>-2</sup> with a concentration of 100 mM of H<sub>2</sub>SO<sub>4</sub>. These results underlined the positive effect of the addition of a supporting electrolyte in the methanol aqueous solution on the electrochemical output that was enhanced. Platinum group metal-free (PGM-free) electrocatalysts based on Fe-N<sub>x</sub>-C type were also tested being insensitive to methanol crossover and oxidation at the cathode. DMFC with Fe-N-C cathode catalysts result in a performance of 21.5 mW cm<sup>-2</sup>. In these operating conditions, the addition of supporting electrolyte does not seem to bring excessive advantage. Short stability tests are presented and an overall assessment of the resistances within the system is also discussed.

## 1. Introduction

Direct Methanol Fuel Cells (DMFCs) show excellent energy performance delivering power output capable of powering e.g. portable electronics or back-up emergency systems [1–3]. The main advantage compared to hydrogen fuel cells is the fact that methanol is in liquid

form and therefore does not present specific problems during transportation [4]. The research in DMFC is mainly devoted in improving anode and cathode electrocatalysts and in parallel optimize the polymer electrolyte membrane [5,6]. Concerning the anode electrocatalysis, great effort is allocated in improving the methanol electrooxidation kinetics by developing Pt alloys capable of mitigating the effect of CO

\* Corresponding author.

E-mail address: [andrea.zaffora@unipa.it](mailto:andrea.zaffora@unipa.it) (A. Zaffora).

<https://doi.org/10.1016/j.jpowsour.2023.232806>

Received 28 October 2022; Received in revised form 13 January 2023; Accepted 9 February 2023

Available online 17 February 2023

0378-7753/© 2023 The Authors. Published by Elsevier B.V. This is an open access article under the CC BY license (<http://creativecommons.org/licenses/by/4.0/>).

poisoning, the intermediate that is formed during MeOH oxidation and poison and deactivate the Pt catalytic centre [7]. Pt–Ru was found to be the most efficient and effective among the Pt-alloy family of electrocatalysts, especially for an equimolar composition and has been largely exploited in the last 30 years [8,9]. Beside of the anode electrocatalyst also the cathode plays a critical role, as the oxygen reduction reaction (ORR) is a sluggish reaction that occurs at large overpotentials that are detrimental to the overall cell efficiency. The ORR electrocatalysis has been largely investigated for its significant role in determining the energy performance of polymer electrolyte membrane (PEM) fuel cells [10–12]. The advancements done in ORR electrocatalysis for PEM fuel cells are often translated within DMFCs systems. Pt based materials are the most used electrocatalysts and typically Pt nanoparticles supported on carbon blacks (Pt/C) can be extremely efficient. Despite being the most used, Pt/C cathode electrocatalysts are not necessarily the most logical solution. So far, typical electrocatalyst loadings in DMFC can be as high as 2–5 mg cm<sup>-2</sup> at the anode and 1 mg cm<sup>-2</sup> at the cathode [13, 14]. Considering a power system capable of delivering reasonable power output (e.g. 100 W), the overall system would have a PGM loading that can easily exceed 4 g and generally 30–40 g per kW are required. This PGM content is not acceptable for this technology significantly affecting the price of the system. Moreover, this large usage introduces treats to the resilience of the technology concerning the dependence of Critical Raw Materials (CRMs) [15]. This aspect has been importantly brought to the public attention by the European Commission that periodically release a list of CRMs [15]. PGMs are among the most critical of those resources, not only for scarcity, but also for the concentration of the resources in the hands of a few countries, a fact that might create issues to the supply chain.

Recently, the use of PGM-free ORR electrocatalysts integrated into the cathode have been proposed for PEMFC. While the performance achieved are not yet at the same level of Pt based materials, it has been demonstrated that these materials can effectively employed in practical systems [16,17]. Among these PGM-free electrocatalysts materials the one belonging to the family of the TM-N<sub>x</sub>-C (x = 2,3,4) which are transition metals (TM) such as Fe, Co, Ni, Mn, et coordinated with nitrogen in pyridinic environment embedded in a carbon matrix and located in the plane or in the edge of the plane are the most promising. These PGM-free electrocatalysts can be single TM (monometallic), bimetallic (TM1-TM2-N-C) or even trimetallic (TM1-TM2-TM3-N-C) [17–22]. Interestingly these PGM-free electrocatalysts offer a huge advantage for DMFC compared to Pt based materials [23]. Indeed, they are not active toward the oxidation of methanol [24,25]. This fact indicates that even in the presence of significant methanol crossover in the cell, no appreciable drop in the open circuit potential of the cell occurs [16]. Remarkably, such drops are one of the major drawbacks of DMFC equipped with Pt cathodes [26].

The DMFC performance is also significantly affected by the concentration of the fuel [27–29]. This is for two reasons: 1) higher concentrations result in higher crossover and 2) methanol concentration may alter the kinetics and the thermodynamics of the electrochemical oxidation [26]. The first point has been already covered when discussing the role of the cathode and has only a negative relationship with concentration. Namely, the higher is the concentration, the higher is the crossover [29]. This results in a drop of the cell efficiency for the loss of the fuel and a further drop in the efficiency for the possible open circuit potential reduction due to the catalytic activity of the cathode toward methanol oxidation. The second point is related to the ratio between methanol and water. The stoichiometric ratio methanol:water should be 17 M, however due to issues related to crossover, the methanol concentration is usually reduced to few M [26]. Moreover, the methanol oxidation has a quite complex reaction mechanism resulting in sluggish kinetics. To accelerate it, higher loading of Pt–Ru/C is used significantly increasing the overall cost of the device without being necessarily efficient [30].

The role of a potential support electrolyte on the performance has

been seldom considered, especially in acidic environment. This role is extremely relevant in alkaline environment where the electrolyte is supported by the addition of hydroxide. For example, in alkaline direct alcohol fuel cells, it has been demonstrated that, for kinetics reasons, ethanol oxidation goes faster for equimolar alcohol and hydroxide concentrations [22,31]. Only a few studies have assessed the effect of H<sub>2</sub>SO<sub>4</sub> as supporting electrolyte on the electrochemical oxidation of methanol [32–34]. Sulfuric acid was typically used as source of sulphate ions approaching the behaviour of sulfonic groups in Nafion® despite dissolved ions in the electrolyte have very different mobility with respect sulfonic groups in a membrane [35]. Recently, kinetics electrochemical studies substituted perchloric acid (HClO<sub>4</sub>) to sulfuric acid because sulphate anions can be strongly adsorbed to the Pt nanoparticles surface hampering methanol adsorption and, therefore, influencing methanol electro oxidation rate. Anyway, Wang and Baltruschat demonstrated that, even if methanol electro oxidation rate is higher in perchloric acid solution than in sulfuric acid one due to stronger adsorption of sulphate anions on Pt surface, current efficiency related to CO<sub>2</sub> production was not significantly influenced [33].

However, the addition of a supporting electrolyte has also been considered for improving the overall ionic conductivity of the system. Li et al. [36] in 2004 used the addition of H<sub>2</sub>SO<sub>4</sub> to the electrolyte of microdirect methanol fuel cell where the electrode was not in mechanical contact with the membrane. In that work, Li and co-workers demonstrated that the addition of H<sub>2</sub>SO<sub>4</sub> was effective to allow the exploitation of extended electrodes in microdevices.

Based on these considerations, we are presenting this research study with the intention of assessing the effectiveness of the addition of sulfuric acid as a supporting electrolyte for methanol fuel composition. The fundamental idea is to evaluate the performance enhancement and the effect that the use of acid fuel may have on the stability of the electrocatalyst, particularly at the cathode. Indeed, as recently reported, the use of cathode PGM-free materials has been proposed as a crossover insensitive alternative to the Pt based materials [23]. Importantly, PGM-free electrocatalysts might show lower stability toward the acidic environment especially in conditions where the acidic groups are not only anchored to the membrane and ionomer but are diluted in the fuel solution.

In this work, an initial screening of Pt/C and Fe–Mn–N–C electrocatalysts is reported using rotating disk electrode (RDE) to evaluate the effect of methanol over the electrocatalytic activity towards ORR. These electrocatalysts are then integrated in the cathode architectures and tested in DMFC with addition of increasing concentration of sulfuric acid as supporting electrolyte. An extensive discussion of the electrochemical performance is presented supported by a meticulous study on the impedance spectroscopy identifying each contribution and relate them to the electrochemistry output. Durability tests were also carried out and reported.

## 2. Materials

### 2.1. Electrocatalyst fabrication

PGM-free electrocatalyst was fabricated using a simplistic methodology to dually functionalize the commercially available carbon black (Ketjenblack EC-600JD, KJ Black) with iron phthalocyanine (FePc) and manganese phthalocyanine (thermos scientific, MnPc). Briefly, 80 wt% of KJ Black was thoroughly mixed with 10 wt% of FePc and 10 wt% of MnPc by subjecting the mixture to a round of ball milling (E<sub>MAX</sub>, Retsch GmbH, Germany) for 1 h at 500 rpm under ambient conditions. Next, the obtained powder was transferred to a clean ceramic boat and pyrolyzed at 600 °C for 1 h while keeping the heating/cooling ramp rates at 300 °C/hr in a split-type horizontal tube furnace (Nabertherm) with a quartz tube. Pyrolysis was carried out under a slightly reducing atmosphere comprising of 5% hydrogen balanced with argon and the flux was maintained at 100 cm<sup>3</sup> min<sup>-1</sup> throughout the process. As the operational

temperature dropped to room temperature, the produced electrocatalyst (KJB-FeMn) was then taken out from the furnace and subsequently analyzed without any further processing.

## 2.2. Electrodes used and membrane electrode assembly integration

For Pt-based electrocatalysts, in-house prepared gas diffusion electrodes were used. The catalytic ink was deposited by spray coating technique onto a commercial gas diffusion layer Sigracet-24 BC (from the SGL group). The catalytic ink was obtained by mixing the electrocatalyst, with 33 wt% of dry Nafion ionomer (5 wt% hydro-alcoholic solution IonPower-LQ1105), and 20 wt% of ammonium carbonate that acts as a pore-former, as described elsewhere [37,38]. For the cathode, a 40% Pt/C (Alfa Aesar) as electrocatalyst and the Pt loading  $0.5 \text{ mg cm}^{-2}$  was used. For the anode, a 60%Pt-Ru/C (Alfa Aesar) was used as electrocatalyst and the Pt loading of  $2.3 \text{ mg cm}^{-2}$  was maintained.

PGM-free electrocatalyst cathode electrode was prepared as follows: the ink was prepared by mixing 150 mg of the as-synthesized catalyst into a solvent containing 2.6 ml (2.41 g) of 5 wt% Nafion and 7 ml of Isopropyl alcohol. The obtained mixture was then subjected to probe sonication for 30 min and subsequently the vial containing ink was placed in the bath sonicator for the next 2 h at ambient conditions. Once the homogenized ink was achieved, 8 ml of it was drop casted on  $25 \text{ cm}^2$  commercial carbon paper gas diffusion layer (Toray TGP-H-120) to make the cathode electrode with loading of  $5 \text{ mg cm}^{-2}$ . In order to allow a fast evaporation of the solvent, the carbon paper was in contact with a hot plate with temperature set at  $80 \text{ }^\circ\text{C}$ . Finally, the cathode electrode was fully dried at  $80 \text{ }^\circ\text{C}$ .

Membrane Electrode Assembly (MEA) was fabricated by mechanical pressing anode, cathode and the proton exchange membrane that was a commercial Nafion® 115. The latter was humidified in deionized water for 15 min before each measurement. Silicone gaskets (with thickness of 0.01") were placed to seal MEA. Cell was assembled by applying a torque of 4 Nm.

## 3. Methods

### 3.1. Surface morphology and chemistry

SEM investigations were performed in a TESCAN GAIA3 2016 dual beam electron microscope equipped with a Triglav electron column. High magnification images (20–500 kx) have been acquired with the column operating in the field immersion mode to collect simultaneously the secondary and primary electrons signals with the in-column detectors secondary and backscattered detectors. For imaging, the electron energy was 5 kV and the working distance approximately 2 mm. Low magnification images have been acquired with the column operating in the analysis mode (no immersion field) to allow a larger field of view and for a better sampling of the catalytic layer for the energy dispersive microanalysis. For EDX analysis, the electron energy was set to 20 kV to allow a significant X-ray emission yield at the Pt L lines. EDX data were collected with an EDAX Octane Elite SDD detector with a Ametek 40 nm Silicon carbide window and a detector active area of  $70 \text{ mm}^2$ .

### 3.2. Electrocatalytic activity testing using rotating disk electrode

For the execution of electrochemical studies, first, a conductive ink of the electrocatalyst was prepared similar to our previously reported methods [39,40]. In brief, 5 mg of the electrocatalyst was mixed with a solvent containing  $985 \mu\text{l}$  of isopropanol (Alfa Aesar) and  $15 \mu\text{l}$  of 5.0 wt % Nafion® D-520 (Alfa Aesar). The suspension was agitated with a probe sonication for 15 min followed by bath sonication for 30 min to obtain a homogenized ink. The oxygen reduction reaction (ORR) was examined through a rotating disk electrode (RDE, Pine WaveVortex) with a three three-electrode symmetry attached to a Pine bipotentiostat. The working electrode was configured by precisely drop-casting the

electrocatalyst ink on the glassy carbon disk of the RDE electrode (E5 series with  $0.1963 \text{ cm}^2$  surface area) with the loading of  $0.6 \text{ mg cm}^{-2}$  for PGM-free and  $0.2 \text{ mg cm}^{-2}$  for Pt/C electrocatalyst. In addition, a saturated calomel electrode (SCE) was used as a reference while the counter electrode was platinum wire. Linear sweep voltammograms (LSVs) were obtained within a potential window of 1000 mV to  $-250 \text{ mV vs SCE}$  in oxygen-rich  $0.5 \text{ M H}_2\text{SO}_4$  electrolyte while rotating RDE at the speed of 1600 rpm. The methanol tolerance of the electrocatalyst was examined by incrementally adding methanol into the base electrolyte from 1 mM to 100 mM concentration. Finally, all the potential values were converted to reversible hydrogen electrode (RHE) potential.

### 3.3. Testing in direct methanol fuel cell

The influence of sulfuric acid and different cathodic electrocatalysts on DMFC performance was studied in a single module fuel cell. ElectroChem Inc. hardware was used and consisted of two gold current collectors and graphite plates with serpentine flow field (used in counter-flow configuration) and an active area of  $1 \text{ cm}^2$ . DMFC characteristics were evaluated by feeding 2 M aqueous solution of methanol at the anode with a flow rate of  $3 \text{ mL min}^{-1}$  and humidified oxygen (99.5% purity, RH = 100%) with a flow rate of  $50 \text{ mL min}^{-1}$  at the cathode (backpressure: 41 kPa). Several concentrations (0.001 M, 0.01 M and 0.1 M) of  $\text{H}_2\text{SO}_4$  in the anodic aqueous solution were tested. Polarization curves were recorded with potentiostatic mode with an acquisition time of 100 s. Every point of the polarization curve was reported as the average of the recorded current values. All DMFC tests were performed at  $70 \text{ }^\circ\text{C}$  using a Parstat 4000 potentiostat (Princeton Applied Research, AMETEK).

Before any test, the cell was activated through a conditioning process. This step is necessary to provide maximum and constant performance over time. Time required for conditioning is closely related to the MEA studied. When Pt/C electrocatalyst was at the cathode side conditioning time was 5 h, while it was 1 h or 5 h for the PGM-free electrocatalysts.

EIS measurements were carried out by superimposing an ac voltage signal of 10 mV to the dc voltage signal of 0.5 V (activation region in the polarization curve) and of 0.25 V (ohmic region in the polarization curve) in the frequency range of 100 kHz to 10 mHz. ZSimpWin software was used to fit the obtained EIS spectra with a suitable equivalent electrical circuit (EEC).

A short stability test was performed to verify the DMFC performance over time. A constant cell voltage of 0.5 V was applied for 10 h, using the same operating conditions as for DMFC testing.

## 4. Results and discussion

### 4.1. The effect of methanol on the ORR kinetics on PGM and PGM-free electrocatalysts

The ORR was investigated using RDE technique and the results are illustrated in Fig. 1 where methanol was stepwise added to the working electrolyte ( $0.5 \text{ M H}_2\text{SO}_4$ ). In the case of Pt/C (Fig. 1a), a categorical oxidation peak can be seen as the methanol was added to the base electrolyte. Increasing the methanol concentration from 1 mM to 100 mM steadily intensified of oxidation peak, indicating the least methanol tolerance of Pt/C. On the other hand, KJB-FeMn did not show a significant poisoning effect due to methanol. However,  $E_{1/2}$  and limiting current density were slightly reduced with subsequent methanol additions. KJB-FeMn electrocatalyst demonstrated a half wave potential ( $E_{1/2}$ ) ca. 0.69 V, 0.66 V, 0.65 V and 0.64 V vs RHE at the methanol concentration of 0 mM, 1 mM, 10 mM and 100 mM, respectively.

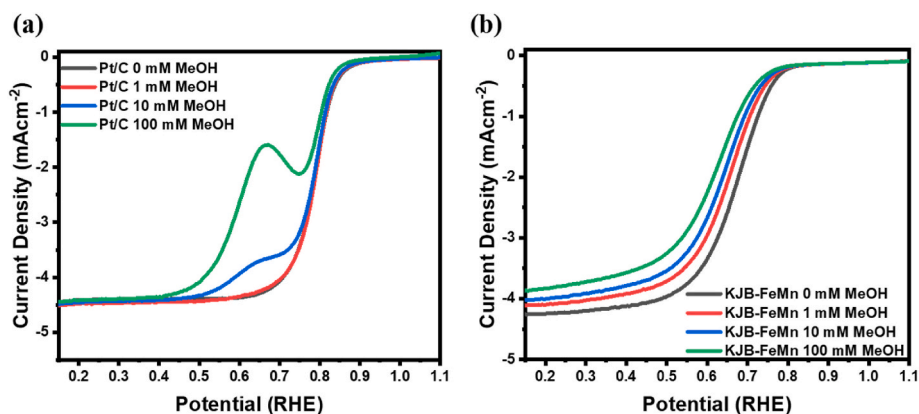


Fig. 1. ORR measurements in  $O_2$ -saturated 0.5 M  $H_2SO_4$  using RDE electrode rotating at 1600 rpm where methanol was sequentially added to the base electrolyte from 1 mM to 100 mM concentration. To obtain LSVs (at  $5 \text{ mV s}^{-1}$ ) electrocatalyst loading on RDE was  $0.2 \text{ mg cm}^{-2}$  for Pt/C (a) while KJB-FeMn (b) was tested with loading of  $0.6 \text{ mg cm}^{-2}$ .

#### 4.2. DMFC testing

##### 4.2.1. Results with Pt electrocatalyst and dependence on $H_2SO_4$ concentration

Fig. 2a and b shows the cell voltage and the power density vs the current density curves related to MEA with Pt and KJB-FeMn electrocatalysts at the cathode, respectively, recorded with different concentrations of  $H_2SO_4$  in the anodic feed methanol solution.

Regarding polarization curves measured using Pt/C electrocatalyst at the cathode, first effect that can be noted about sulfuric acid presence in methanol aqueous solution is that OCV value slightly increased, from  $\approx 650 \text{ mV}$  without  $H_2SO_4$  to  $\approx 710 \text{ mV}$  with a 0.1 M  $H_2SO_4$  concentration. This value is anyway far from electromotive force (emf) value, i.e. 1210 mV, due to the high methanol crossover from the anodic to the cathodic side that the polymeric membrane utilized, Nafion® 115, experienced. Methanol crossover creates mixed potentials responsible for the lower value recorded compared to the theoretical value. It can be noticed that a gradual increase in the peak of power density was obtained as the concentration of sulfuric acid in the anode feed increased; an overall increase of 64% can be estimated with the addition of a concentration of 0.1 M  $H_2SO_4$  compared with 2 M methanol aqueous solution, reaching  $115 \text{ mW cm}^{-2}$  as maximum power density peak.

It is noteworthy to mention that the major effect of  $H_2SO_4$  presence was on the overall ionic conductivity of the cell. In fact, it could be noted that the slope of the linear part of the polarization curves (ohmic region) decreased with increasing sulfuric acid concentration in the methanol aqueous solution anodic feed.

##### 4.2.2. Results with PGM-free cathode electrocatalyst

###### 4.2.2.1. Effect of conditioning time. The effect of conditioning time was

evaluated for KJB-FeMn (i.e. PGM-free) electrocatalyst. In contrast to Pt electrocatalyst, conditioning process resulted to be detrimental for KJB-FeMn performance output. In fact, initial OCV and power density peak values ( $685 \text{ mV}$  and  $18 \text{ mW cm}^{-2}$ , respectively) decreased after 5 h conditioning, being  $645 \text{ mV}$  and  $14 \text{ mW cm}^{-2}$ , respectively (see Fig. S1). This result could be explained by considering possible dissolution phenomena of the metallic centers (Fe and Mn) that can happen in acidic conditions, as those in DMFC, since these metals are not thermodynamically stable in acid solutions [41].

###### 4.2.2.2. Effect of addition of sulfuric acid.

As it can be noted from polarization curves reported in Fig. 2b, recorded OCV values were not far from those recorded with Pt electrocatalyst at the cathode. OCV value is directly related to the sensitivity of the PGM-free electrocatalyst to methanol crossover and its electrooxidation. It is reported in literature that methanol crossover decreases the performance of the ORR, by limiting oxygen availability on the active sites. Moreover, it has been proposed that the MOR at the cathode occurs through an electrochemical mechanism, thus increasing the cathode overpotential [42]. In the case of KJB-FeMn electrocatalyst, ORR is also characterized by a higher charge transfer resistance with respect to the Pt/C case. Therefore, close OCV values can be explained by considering a lower sensitivity to methanol crossover compensated by a more sluggish ORR. It is also noteworthy to mention that huge differences in OCV values using PGM-based and PGM-free electrocatalysts can be typically found when methanol concentration higher than 2 M are used [43].

Regarding power density values, they were much lower by using KJB-FeMn catalyst, being the maximum  $21.5 \text{ mW cm}^{-2}$  with 0.1 M  $H_2SO_4$  concentration in methanol aqueous solution.

Differently than in the case of Pt, it is important to note that, both OCV values and power densities, did not show a significant dependence

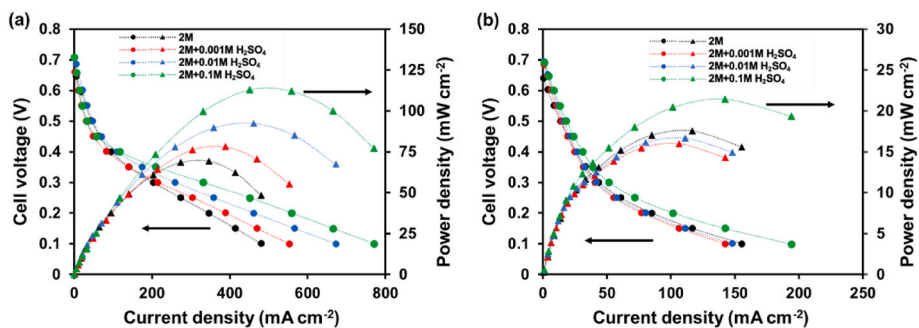


Fig. 2. Polarization curves and power density curves recorded at  $70 \text{ }^\circ\text{C}$  with different concentrations of sulfuric acid in the anodic feed (2 M aqueous methanol solution). (a) Pt catalyst and (b) KJB-FeMn catalyst at the cathode.

on the presence of sulfuric acid in anodic feed. By looking at the polarization curves, it is worth noting that these worst performances were mainly due to major activation losses linked to KJB-FeMn at the cathode with respect to those estimated by using Pt for the oxygen reduction reaction. Nevertheless, a power density peak value of  $21.5 \text{ mW cm}^{-2}$  is considerable if compared to data reported in literature for PGM-free ORR electrocatalyst used in DMFC with comparable operating conditions [21,22,24,44]. These results demonstrate the potentiality of this electrocatalyst.

#### 4.2.3. EIS analysis

Previous reported results can be also confirmed and rationalized by looking at EIS spectra shown in Fig. 3a–d recorded for Pt and KJB-FeMn electrocatalysts, without and with sulfuric acid (0.1 M) at the anode, at 0.5 V as cell voltage.

Electrochemical behavior of DMFCs was modelled by considering the equivalent electrical circuit (EEC) reported in the inset of Fig. 3a. EEC comprised ohmic resistance,  $R_{\Omega}$ , taking into account membrane (Nafion® 115) resistance and all the other ohmic resistances (e.g. methanol aqueous solution resistance), in series with two more complex circuits, modelling anode and cathode and respective reactions kinetics. In fact, for both electrodes, a parallel between  $R_{ct}$  and  $Q$  was considered, representing the charge transfer resistance related to the specific electrochemical reaction and a constant phase element used to model for a non ideal double layer capacitance, respectively. In the case of EIS spectra recorded at a cell voltage of 0.25 V, to model anode and its reaction kinetics, a series between an inductance and a resistance was added to the EEC used (see Fig. S3). In fact, an inductance was needed to model the adsorption of CO species (preferentially) on Pt that is involved in the complex multistep reaction mechanism of methanol oxidation [45]. Ohmic resistance and kinetics fitting parameters of EIS spectra recorded at 0.5 V and 0.25 V are reported in Table 1, whilst all the fitting parameters regarding all the spectra related to the cell operating with both electrocatalyst types and sulfuric acid concentrations are reported in Table S1 and Table S2.

$R_{ct,C}$  resulted to be one order of magnitude higher with respect to  $R_{ct,A}$  when KJB-FeMn electrocatalyst was used for cathodic reaction. In turn,  $R_{ct,A}$  resulted to be one order of magnitude higher with respect to

$R_{ct,C}$  when Pt electrocatalyst was used for cathodic reaction, confirming that higher activation overpotential values are needed to activate ORR when KJB-FeMn electrocatalyst was used.  $R_{ct,C}$  was determined by comparing the obtained values with those reported in previous studies related to  $H_2$ -fed low T fuel cells for ORR [46]. It is noteworthy to mention that, when Pt was used at cathode, increasing the concentration of sulfuric acid led to a decrease of  $R_{ct,A}$  and  $R_{ct,C}$  at higher current density values (i.e. dc cell voltage = 0.25 V, see Table 1b). It is also noteworthy to mention that, at 0.25 V, the overvoltage values related to both electrochemical reactions, which can be estimated as  $emf - IR$ , are as high as to have fully activated reactions, resulting in comparable values of  $R_{ct,C}$  and  $R_{ct,A}$ . This can be also explained by considering a possible change in the rate determining step for electrooxidation of methanol at this so high overvoltage value, making fast an intrinsic sluggish reaction as MOR is. On the contrary, no clear trend was assessed when KJB-FeMn was used by changing the  $H_2SO_4$  concentration, in agreement with polarization curves shown in Fig. 2b. In fact, in the latter case, the overall performance is controlled by the worse kinetics at the cathode, thus the effect of sulfuric acid presence is not so evident.

Results of short stability test, carried out at 0.5 V for 10 h, for both DMFCs employing Pt and KJB-FeMn electrocatalysts at the cathode are reported in Figs. 4 and 5, respectively. Cell voltage of 0.5 V was chosen since it was reported that a constant cell voltage of 0.5 V is the most severe condition to test DMFC components [47] and, recently, 0.5 V has been indicated as the operating cell voltage for the maximum efficiency of a DMFC [48].

When Pt was used as electrocatalyst at the cathode (see Fig. 4), regardless on the anodic feed composition, current density value reached an almost constant value after  $\sim 30$  min whilst transitory phase resulted to be longer when KJB-FeMn electrocatalyst was used (see Fig. 5) with a lower stationary current density value.

After short stability test employing Pt (i.e. after 10 h of constant polarization), power density value decreased to  $105 \text{ mW cm}^{-2}$  (see inset of Fig. 4) when sulfuric acid was present in the anodic feed whilst it decreased to  $50 \text{ mW cm}^{-2}$  (see inset of Fig. 4) when no sulfuric acid was used. This means a decrease of  $\sim 10\%$  in power density value after short stability test in both cases, i.e. without and with sulfuric acid in anodic feed. A possible reason for the degradation in cell performance could be Pt and/or Ru leaching from the anodic electrocatalyst.

After short stability test employing KJB-FeMn, power density value decreased to  $15 \text{ mW cm}^{-2}$  (see inset of Fig. 5) when sulfuric acid was present in the anodic feed whilst it decreased to  $12 \text{ mW cm}^{-2}$  (see inset of Fig. 5) when no sulfuric acid was used. This means a decrease of  $\sim 30\%$  in power density value after short stability test in both cases, i.e. without and with sulfuric acid in anodic feed, respectively. For KJB-FeMn electrocatalyst, a worse performance is supposed to be due to Fe and/or Mn dissolution.

#### 4.2.4. Stability investigation by SEM analysis

To assess the effect of the addition of  $H_2SO_4$  on the stability of the anode and cathode materials, we performed the SEM imaging on the electrodes after the acquisition of the polarization curves. Fig. 6 shows the high magnification images of the electrocatalysts integrated into the cathode catalyst layer after DMFC polarization curves with 2 M  $CH_3OH$  and 2 M  $CH_3OH + 0.1 \text{ M } H_2SO_4$ . Data for the cells with 0.001 M and 0.01 M are reported in Figs. S2a–h. We observed that in the cell equipped with both the PGM and the PGM-free materials the electrocatalyst show no apparent change of the morphology. A rule of thumb quantitative estimation done by EDX microanalysis (see Table 2) show that the Pt–Ru ratio in the anode after the polarization experiments did not change with the addition of sulfuric acid, suggesting the robustness, at least for the short term stability, of the system against the anodic stress. These findings are in agreement with what observed with the short stability tests, where the current output at an applied potential of 0.5 V does not show dependence on the  $H_2SO_4$  concentration in a 10 h timespan.

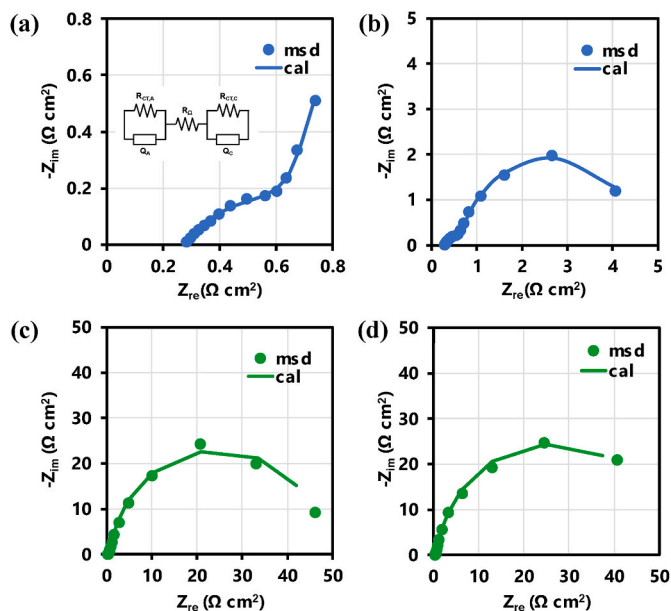
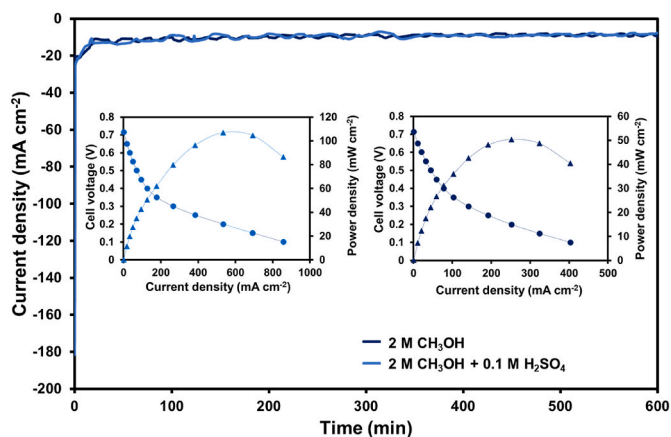


Fig. 3. EIS spectra recorded at 0.5 V with Pt at cathode a) without and b) with sulfuric acid (0.1 M) in the anodic feed. EIS spectra recorded at 0.5 V with KJB-FeMn at cathode c) without and d) with sulfuric acid (0.1 M) in the anodic feed. Continuous line: fitting line.

**Table 1**

Ohmic resistance and kinetics fitting parameters of EIS spectra recorded at a) 0.5 V and b) 0.25 V with several sulfuric acid concentrations with Pt and KJB-FeMn at the cathode.

a) Cell voltage = 0.5 V								
	Pt (cathode) - PtRu (anode)				KJB-FeMn (cathode) - PtRu (anode)			
	2 M	2 M + 0.001 M H <sub>2</sub> SO <sub>4</sub>	2 M + 0.01 M H <sub>2</sub> SO <sub>4</sub>	2 M + 0.1 M H <sub>2</sub> SO <sub>4</sub>	2 M	2 M + 0.001 M H <sub>2</sub> SO <sub>4</sub>	2 M + 0.01 M H <sub>2</sub> SO <sub>4</sub>	2 M + 0.1 M H <sub>2</sub> SO <sub>4</sub>
R <sub>Ω</sub> (Ω cm <sup>2</sup> )	0.28	0.32	0.29	0.28	0.25	0.25	0.25	0.28
R <sub>ct,C</sub> (Ω cm <sup>2</sup> )	0.45	0.59	0.59	0.42	44.6	46.8	49.0	47.0
R <sub>ct,A</sub> (Ω cm <sup>2</sup> )	4.26	5.44	4.70	4.32	3.29	4.38	4.60	4.20
b) Cell Voltage = 0.25 V.								
	Pt (cathode) - PtRu (anode)				KJB-FeMn (cathode) - PtRu (anode)			
	2 M	2 M + 0.001 M H <sub>2</sub> SO <sub>4</sub>	2 M + 0.01 M H <sub>2</sub> SO <sub>4</sub>	2 M + 0.1 M H <sub>2</sub> SO <sub>4</sub>	2 M	2 M + 0.001 M H <sub>2</sub> SO <sub>4</sub>	2 M + 0.01 M H <sub>2</sub> SO <sub>4</sub>	2 M + 0.1 M H <sub>2</sub> SO <sub>4</sub>
R <sub>Ω</sub> (Ω cm <sup>2</sup> )	0.27	0.27	0.28	0.25	0.28	0.26	0.25	0.24
R <sub>ct,C</sub> (Ω cm <sup>2</sup> )	0.40	0.26	0.21	0.16	7.00	7.48	6.15	4.79
R <sub>ct,A</sub> (Ω cm <sup>2</sup> )	0.45	0.25	0.22	0.20	0.45	0.20	0.14	0.16



**Fig. 4.** Short stability tests (constant cell voltage = 0.5 V), using aqueous methanol solution at anode without and with sulfuric acid, related to DMFCs employing Pt electrocatalyst at the cathode. Inset: polarization curves recorded after the short stability tests.

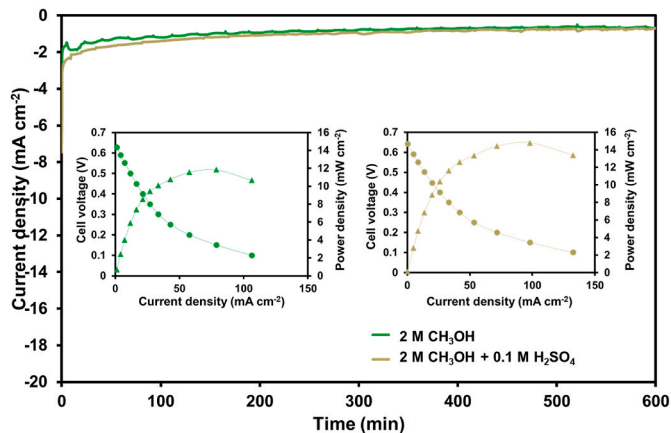


**Fig. 5.** Short stability tests (constant cell voltage = 0.5 V), using aqueous methanol solution at anode without and with sulfuric acid, related to DMFCs employing KJB-FeMn electrocatalyst at the cathode. Inset: polarization curves recorded after the short stability tests.

## 5. Conclusions

In this work, we have explored the addition of H<sub>2</sub>SO<sub>4</sub> as a supporting electrolyte for direct methanol fuel cells with the purpose to increase the

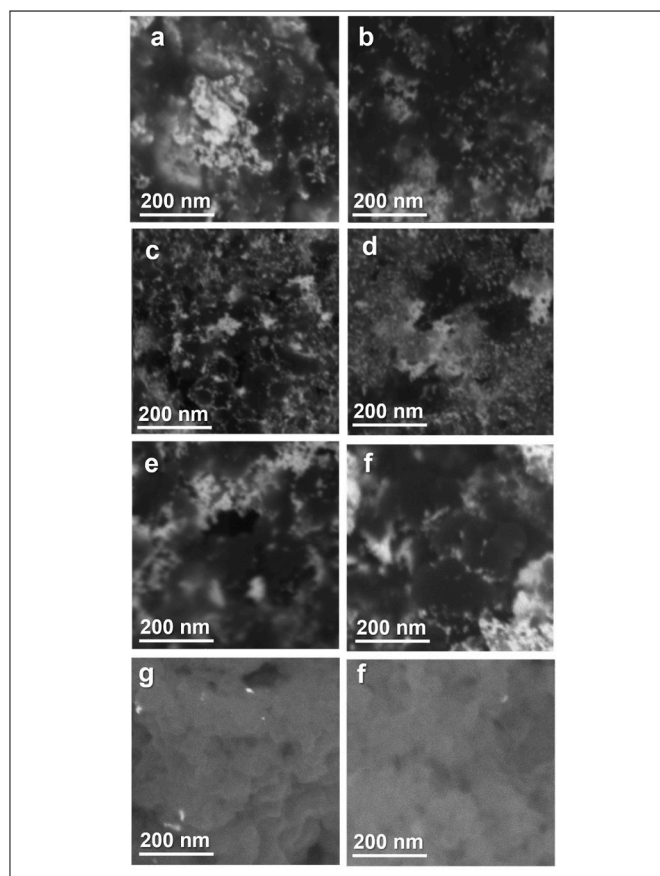


**Fig. 6.** High resolution SEM images (500kx) of the electrodes of the cell equipped with Pt cathode (a–d) and KJB-FeMn cathodes (e–h). a) Pt–Ru anode after polarization tests in 2 M CH<sub>3</sub>OH; b) Pt–Ru anode after polarization tests in 2 M CH<sub>3</sub>OH + 0.1 M H<sub>2</sub>SO<sub>4</sub>; c) Pt cathode after polarization tests in 2 M CH<sub>3</sub>OH; d) Pt cathode after polarization tests in 2 M CH<sub>3</sub>OH + 0.1 M H<sub>2</sub>SO<sub>4</sub>; e) Pt–Ru anode after polarization tests in 2 M CH<sub>3</sub>OH; f) Pt–Ru anode after polarization tests in 2 M CH<sub>3</sub>OH + 0.1 M H<sub>2</sub>SO<sub>4</sub>; g) KJB-FeMn cathode after polarization tests in 2 M CH<sub>3</sub>OH; h) KJB-FeMn cathode after polarization tests in 2 M CH<sub>3</sub>OH + 0.1 M H<sub>2</sub>SO<sub>4</sub>.

power density of the devices. We showed that the addition of 0.1 M H<sub>2</sub>SO<sub>4</sub> to a cell equipped with a Pt–Ru anode and a Pt cathode produce an outstanding 64% increase of the power output. Remarkably at a cell potential of 0.25 V the current density increases from 0.27 to 0.45 A cm<sup>-2</sup>. EIS data showed that such a huge variation is due to both a reduction in the cell resistance and the improvement of the anode

**Table 2**

Pt/Ru ratio (wt.%) after the DMFC polarization experiments. Initial Pt/Ru ratio (wt.%) = 1.77.

Electrocatalysts	2 M	2 M + 0.001 M H <sub>2</sub> SO <sub>4</sub>	2 M + 0.01 M H <sub>2</sub> SO <sub>4</sub>	2 M + 0.1 M H <sub>2</sub> SO <sub>4</sub>
Pt/Ru (Pt Cathode)	1.43	1.40	1.36	1.39
Pt/Ru (KJB-FeMn Cathode)	1.42	1.39	1.43	1.37

kinetics. As the frontier is to reduce the amount of Pt as much as possible to lower the impact on critical raw materials and to avoid potential drops due to methanol crossover, we explored the addition of H<sub>2</sub>SO<sub>4</sub> to the same DMFC equipped with a PGM-free cathode consisting of a pyrolyzed carbon added with TM-N<sub>x</sub> catalytic centers using bimetallic TMs such as Fe and Mn. For such a cell, the power density moved from 18 mW cm<sup>-2</sup> to 21.5 mW cm<sup>-2</sup> with a 20% increase. The results obtained in this case are less predominant than that of the cell equipped with the Pt/C cathode. We ascribed this finding to the higher cathode charge transfer resistance that, according to EIS data, looks the most limiting factor for defining the cell performance, especially at the lowest overpotentials. Nonetheless, we can conclude that adding H<sub>2</sub>SO<sub>4</sub> as a supporting electrolyte has a beneficial effect to the energy performance that results in a significant increase of the weight and volume power density of the devices.

While the performance of the system equipped with the PGM-free cathode are in line with what reported in the state of the art for DMFC, we observed that the maximum power density of the DMFC equipped with Pt/C cathodes is roughly five times higher. Accordingly, we can conclude that considering that the Pt loading at the anode is 2.3 mg cm<sup>-2</sup>, the Pt saving produced by its elimination at the cathode is not justified as to achieve the same power output the PGM-free cell must be five time larger. Eventually, considering that in PGM-free systems the kinetics is mostly driven by the cathode, a catalyst loading reduction at the anode could be considered.

The addition of H<sub>2</sub>SO<sub>4</sub> might rise concern on the stability of the performance. We explored this aspect by recording potentiostatic curves for 10 h to assess the short term stability. A comparison of the stability between the system fueled with bare CH<sub>3</sub>OH and CH<sub>3</sub>OH + 0.1 M H<sub>2</sub>SO<sub>4</sub> did not show significant difference in the performance decrease. An analysis of the catalyst morphology and composition by SEM and EDX microanalysis also showed that the catalyst layers did not show significant change in the composition between the cell equipped with supported and unsupported electrolytes.

In conclusion, our finding shows that the addition of small amount of H<sub>2</sub>SO<sub>4</sub> to the fuel of DMFC can increase the performance of the system defining a potential approach to the increase of the energy performance of such devices.

#### CRediT authorship contribution statement

**Elena Giordano:** Conceptualization, Formal analysis, Investigation, Data curation, Writing – original draft, Visualization. **Enrico Berretti:** Investigation. **Laura Capozzoli:** Investigation, Writing – review & editing. **Alessandro Lavacchi:** Conceptualization, Methodology, Resources, Writing – original draft, Writing – review & editing, Supervision, Funding acquisition. **Mohsin Muhyuddin:** Investigation, Writing – original draft, Visualization. **Carlo Santoro:** Conceptualization, Methodology, Resources, Writing – original draft, Writing – review & editing, Supervision, Funding acquisition. **Irene Gatto:** Investigation, Resources, Writing – review & editing. **Andrea Zaffora:** Conceptualization, Methodology, Formal analysis, Data curation, Writing – original draft, Writing – review & editing, Visualization, Supervision. **Monica Santamaria:** Conceptualization, Methodology, Resources, Writing – review & editing, Supervision, Funding acquisition, Project administration.

#### Declaration of competing interest

The authors declare the following financial interests/personal relationships which may be considered as potential competing interests: Carlo Santoro reports financial support was provided by Government of Italy Ministry of Education University and Research. Andrea Zaffora reports financial support was provided by Government of Italy Ministry of Education University and Research. Alessandro Lavacchi reports financial support was provided by Government of Italy Ministry of Education University and Research. Laura Capozzoli reports financial support was provided by Government of Italy Ministry of Education University and Research. Enrico Berretti reports financial support was provided by Government of Italy Ministry of Education University and Research.

#### Data availability

Data will be made available on request.

#### Acknowledgements

Carlo Santoro would like to thank the support from the Italian Ministry of Education, University and Research (MIUR) through the “Rita Levi Montalcini 2018” fellowship (Grant number PGR18MAZLI). Andrea Zaffora acknowledges support from the Italian Ministry of University and Research (MUR) within the program PON R&I 2014-2020—Attraction and International Mobility (AIM)—project no. AIM1845825-3. Alessandro Lavacchi, Laura Capozzoli and Enrico Berretti acknowledge support from the Italian Ministry of Education, University and Research (MIUR) within the program AMPERE - FISIR2019\_01294.

#### Appendix A. Supplementary data

Supplementary data to this article can be found online at <https://doi.org/10.1016/j.jpowsour.2023.232806>.

#### References

- [1] A.S. Aricò, S. Srinivasan, V. Antonucci, DMFCs: from fundamental aspects to technology development, *Fuel Cell*. (2001) 133–161, <https://doi.org/10.1002/1615-6854>. July.
- [2] U.A. Icardi, S. Specchia, G.J.R. Fontana, G. Saracco, V. Specchia, Compact direct methanol fuel cells for portable application, *J. Power Sources* 176 (2008) 460–467, <https://doi.org/10.1016/j.jpowsour.2007.08.048>.
- [3] E.H. Yu, U. Krewer, K. Scott, Principles and materials aspects of direct alkaline alcohol fuel cells, *Energies* 3 (2010) 1499–1528, <https://doi.org/10.3390/EN3081499>.
- [4] R.G. Akay, A.B. Yurtcan, in: *Direct Liquid Fuel Cells: Fundamentals, Advances and Technical Roadmaps*, Academic Press, 2021.
- [5] Y. Zuo, W. Sheng, W. Tao, Z. Li, Direct methanol fuel cells system—A review of dual-ole electrocatalysts for oxygen reduction and methanol oxidation, *J. Mater. Sci. Technol.* 114 (2022) 29–41, <https://doi.org/10.1016/j.jmst.2021.10.031>.
- [6] A. Sajid, E. Pervaiz, H. Ali, T. Noor, M.M. Baig, A perspective on development of fuel cell materials: electrodes and electrolyte, *Int. J. Energy Res.* 46 (2022) 6953–6988, <https://doi.org/10.1002/ER.7635>.
- [7] A. Yuda, A. Ashok, A. Kumar, A comprehensive and critical review on recent progress in anode catalyst for methanol oxidation reaction, *Catal. Rev.* 64 (2022) 126–228, <https://doi.org/10.1080/01614940.2020.1802811>.
- [8] H. Liu, C. Song, L. Zhang, J. Zhang, H. Wang, D.P. Wilkinson, A review of anode catalysis in the direct methanol fuel cell, *J. Power Sources* 155 (2006) 95–110, <https://doi.org/10.1016/j.jpowsour.2006.01.030>.
- [9] M. Wala, W. Simka, Effect of anode material on electrochemical oxidation of low molecular weight alcohols—a review, *Molecules* 26 (2021) 2144, <https://doi.org/10.3390/MOLECULES26082144>.
- [10] Y.J. Wang, N. Zhao, B. Fang, H. Li, X.T. Bi, H. Wang, Carbon-supported Pt-based alloy electrocatalysts for the oxygen reduction reaction in polymer electrolyte membrane fuel cells: particle size, shape, and composition manipulation and their impact to activity, *Chem. Rev.* 115 (2015) 3433–3467, [https://doi.org/10.1021/CR500519C/ASSET/IMAGES/LARGE/CR-2014-00519C\\_0007](https://doi.org/10.1021/CR500519C/ASSET/IMAGES/LARGE/CR-2014-00519C_0007). JPEG.
- [11] M. Shao, Q. Chang, J.P. Dodelet, R. Chenitz, Recent advances in electrocatalysts for oxygen reduction reaction, *Chem. Rev.* 116 (2016) 3594–3657, [https://doi.org/10.1021/ACS.CHEMREV.5B00462/ASSET/IMAGES/LARGE/CR-2015-00462U\\_0038](https://doi.org/10.1021/ACS.CHEMREV.5B00462/ASSET/IMAGES/LARGE/CR-2015-00462U_0038). JPEG.

- [12] K. Kodama, T. Nagai, A. Kuwaki, R. Jinnouchi, Y. Morimoto, Challenges in applying highly active Pt-based nanostructured catalysts for oxygen reduction reactions to fuel cell vehicles, *Nat. Nanotechnol.* 16 (2) (2021) 140–147, <https://doi.org/10.1038/s41565-020-00824-w>, 16 (2021).
- [13] Q. Shu, Z. Xia, W. Wei, X. Xu, R. Sun, R. Deng, Q. Yang, H. Zhao, S. Wang, G. Sun, Controllable unzipping of carbon nanotubes as advanced Pt catalyst supports for oxygen reduction, *ACS Appl. Energy Mater.* 2 (2019) 5446–5455, <https://doi.org/10.1021/ACSAPM.9B00506>, *ASSET/IMAGES/LARGE/AE-2019-00506X\_0006*. JPEG.
- [14] Q. Shi, Y. He, X. Bai, M. Wang, D.A. Cullen, M. Lucero, X. Zhao, K.L. More, H. Zhou, Z. Feng, Y. Liu, G. Wu, Methanol tolerance of atomically dispersed single metal site catalysts: mechanistic understanding and high-performance direct methanol fuel cells, *Energy Environ. Sci.* 13 (2020) 3544–3555, <https://doi.org/10.1039/D0EE01968B>.
- [15] Critical raw materials, (n.d.). [https://single-market-economy.ec.europa.eu/sectors/raw-materials/areas-specific-interest/critical-raw-materials\\_en](https://single-market-economy.ec.europa.eu/sectors/raw-materials/areas-specific-interest/critical-raw-materials_en) (accessed October 24, 2022).
- [16] C. lo Vecchio, A. Serov, H. Romero, A. Lubers, B. Zulevi, A.S. Aricò, V. Baglio, Commercial platinum group metal-free cathodic electrocatalysts for highly performed direct methanol fuel cell applications, *J. Power Sources* 437 (2019), 226948, <https://doi.org/10.1016/J.JPOWSOUR.2019.226948>.
- [17] C. lo Vecchio, A. Serov, M. Dicome, B. Zulevi, A.S. Aricò, V. Baglio, Investigating the durability of a direct methanol fuel cell equipped with commercial Platinum Group Metal-free cathodic electro-catalysts, *Electrochim. Acta* 394 (2021), 139108, <https://doi.org/10.1016/J.ELECTACTA.2021.139108>.
- [18] D. Sebastián, V. Baglio, A.S. Aricò, A. Serov, P. Atanassov, Performance analysis of a non-platinum group metal catalyst based on iron-aminoantipyrine for direct methanol fuel cells, *Appl. Catal., B* 182 (2016) 297–305, <https://doi.org/10.1016/J.APCATB.2015.09.043>.
- [19] D. Sebastián, A. Serov, K. Artyushkova, P. Atanassov, A.S. Aricò, V. Baglio, Performance, methanol tolerance and stability of Fe-aminobenzimidazole derived catalyst for direct methanol fuel cells, *J. Power Sources* 319 (2016) 235–246, <https://doi.org/10.1016/J.JPOWSOUR.2016.04.067>.
- [20] D. Sebastián, A. Serov, K. Artyushkova, J. Gordon, P. Atanassov, A.S. Aricò, V. Baglio, High performance and cost-effective direct methanol fuel cells: Fe-N-C methanol-tolerant oxygen reduction reaction catalysts, *ChemSusChem* 9 (2016) 1986–1995, <https://doi.org/10.1002/SSC.201600583>.
- [21] L. Osmieri, R. Escudero-Cid, A.H.A. Monteverde Videla, P. Ocón, S. Specchia, Performance of a Fe-N-C catalyst for the oxygen reduction reaction in direct methanol fuel cell: cathode formulation optimization and short-term durability, *Appl. Catal., B* 201 (2017) 253–265, <https://doi.org/10.1016/J.APCATB.2016.08.043>.
- [22] L. Osmieri, R. Escudero-Cid, M. Armandi, A.H.A. Monteverde Videla, J.L. García Fierro, P. Ocón, S. Specchia, Fe-N/C catalysts for oxygen reduction reaction supported on different carbonaceous materials. Performance in acidic and alkaline direct alcohol fuel cells, *Appl. Catal., B* 205 (2017) 637–653, <https://doi.org/10.1016/J.APCATB.2017.01.003>.
- [23] E. Berretti, M. Longhi, P. Atanassov, D. Sebastián, C. lo Vecchio, V. Baglio, A. Serov, A. Marchionni, F. Vizza, C. Santoro, A. Lavacchi, Platinum group metal-free Fe-based (FeNC) oxygen reduction electrocatalysts for direct alcohol fuel cells, *Curr. Opin. Electrochem.* 29 (2021), 100756, <https://doi.org/10.1016/J.COLEEC.2021.100756>.
- [24] I. Martinaiou, A.H.A. Monteverde Videla, N. Weidler, M. Kübler, W.D.Z. Wallace, S. Paul, S. Wagner, A. Shahraei, R.W. Stark, S. Specchia, U.I. Kramm, Activity and degradation study of an Fe-N-C catalyst for ORR in direct methanol fuel cell (DMFC), *Appl. Catal., B* 262 (2020), 118217, <https://doi.org/10.1016/J.APCATB.2019.118217>.
- [25] W. da Silva Freitas, B. Mecheri, C. lo Vecchio, I. Gatto, V. Baglio, V.C.A. Ficca, A. Patra, E. Placidi, A. D'Epifanio, Metal-organic-framework-derived electrocatalysts for alkaline polymer electrolyte fuel cells, *J. Power Sources* 550 (2022), 232135, <https://doi.org/10.1016/J.JPOWSOUR.2022.232135>.
- [26] D. Sebastián, A. Serov, I. Matanovic, K. Artyushkova, P. Atanassov, A.S. Aricò, V. Baglio, Insights on the extraordinary tolerance to alcohols of Fe-N-C cathode catalysts in highly performing direct alcohol fuel cells, *Nano Energy* 34 (2017) 195–204, <https://doi.org/10.1016/J.NANOEN.2017.02.039>.
- [27] J.G. Liu, T.S. Zhao, R. Chen, C.W. Wong, The effect of methanol concentration on the performance of a passive DMFC, *Electrochem. Commun.* 7 (2005) 288–294, <https://doi.org/10.1016/J.ELECOM.2005.01.011>.
- [28] A. Casalegno, R. Marchesi, DMFC performance and methanol cross-over: experimental analysis and model validation, *J. Power Sources* 185 (2008) 318–330, <https://doi.org/10.1016/J.JPOWSOUR.2008.06.071>.
- [29] A. Casalegno, C. Santoro, F. Rinaldi, R. Marchesi, Low methanol crossover and high efficiency direct methanol fuel cell: the influence of diffusion layers, *J. Power Sources* 196 (2011) 2669–2675, <https://doi.org/10.1016/J.JPOWSOUR.2010.11.050>.
- [30] N. Kakati, J. Maiti, S.H. Lee, S.H. Jee, B. Viswanathan, Y.S. Yoon, Anode catalysts for direct methanol fuel cells in acidic media: do we have any alternative for Pt or Pt-Ru? *Chem. Rev.* 114 (2014) 12397–12429, <https://doi.org/10.1021/CR400389F>, *ASSET/IMAGES/LARGE/CR-2013-00389F\_0031*. JPEG.
- [31] L. Osmieri, R. Escudero-Cid, A.H.A. Monteverde Videla, P. Ocón, S. Specchia, Application of a non-noble Fe-N-C catalyst for oxygen reduction reaction in an alkaline direct ethanol fuel cell, *Renew. Energy* 115 (2018) 226–237, <https://doi.org/10.1016/J.RENENE.2017.08.062>.
- [32] E.P.M. Leiva, M.C. Giordano, Multiple current components for methanol electroadsorption and electro-oxidation at platinum in acidic solutions, *J. Electroanal. Chem.* 158 (1983) 115–130.
- [33] H. Wang, H. Baltruschat, DEMS study on methanol oxidation at poly- and monocrystalline platinum electrodes: the effect of anion, temperature, surface structure, Ru adatom, and potential, *J. Phys. Chem. C* 111 (2007) 7038–7048, <https://doi.org/10.1021/jp068328n>.
- [34] A. Santasalo, F.J. Vidal-Iglesias, J. Solla-Gullón, A. Berná, T. Kallio, J.M. Felii, Electrooxidation of methanol and 2-propanol mixtures at platinum single crystal electrodes, *Electrochim. Acta* 54 (2009) 6576–6583, <https://doi.org/10.1016/j.electacta.2009.06.033>.
- [35] L. Osmieri, R. Escudero-Cid, S. Tuomi, K. Jalkanen, K. Kontturi, T. Kallio, The correlation of electrochemical and fuel cell results for alcohol oxidation in acidic and alkaline media, *Electrochim. Acta* 87 (2013) 730–738, <https://doi.org/10.1016/j.electacta.2012.09.100>.
- [36] J. Li, C. Moore, P.A. Kohl, Investigation of acidic methanol solution as a fuel for microchannel fuel cells, *J. Power Sources* 138 (2004) 211–215, <https://doi.org/10.1016/J.JPOWSOUR.2004.06.048>.
- [37] I. Gatto, A. Stassi, E. Passalacqua, A.S. Aricò, An electro-kinetic study of oxygen reduction in polymer electrolyte fuel cells at intermediate temperatures, *Int. J. Hydrogen Energy* 38 (2013) 675–681, <https://doi.org/10.1016/J.IJHYDENE.2012.05.155>.
- [38] I. Gatto, A. Carbone, A. Saccà, E. Passalacqua, C. Oldani, L. Merlo, D. Sebastián, A. S. Aricò, V. Baglio, Increasing the stability of membrane-electrode assemblies based on Aquivion® membranes under automotive fuel cell conditions by using proper catalysts and ionomers, *J. Electroanal. Chem.* 842 (2019) 59–65, <https://doi.org/10.1016/J.JELECHEM.2019.04.058>.
- [39] M. Muhyuddin, N. Zocche, R. Lorenzi, C. Ferrara, F. Poli, F. Soavi, C. Santoro, Valorization of the inedible pistachio shells into nanoscale transition metal and nitrogen codoped carbon-based electrocatalysts for hydrogen evolution reaction and oxygen reduction reaction, *Mater. Res. New. Sustain. Energy* 11 (2022) 131–141, <https://doi.org/10.1007/S40243-022-00212-5>, *FIGURES/5*.
- [40] M. Muhyuddin, J. Filippi, L. Zoia, S. Bonizzoni, R. Lorenzi, E. Berretti, L. Capozzoli, M. Bellini, C. Ferrara, A. Lavacchi, C. Santoro, Waste face surgical mask transformation into crude oil and nanostructured electrocatalysts for fuel cells and electrolyzers, *ChemSusChem* 15 (2022), e202102351, <https://doi.org/10.1002/SSC.202102351>.
- [41] M. Pourbaix, *Atlas of Electrochemical Equilibria in Aqueous Solutions*, Pergamon Press, Oxford, UK, 1966.
- [42] M. Zago, A. Bisello, A. Baricci, C. Rabissi, E. Brightman, G. Hinds, A. Casalegno, On the actual cathode mixed potential in direct methanol fuel cells, *J. Power Sources* 325 (2016) 714–722, <https://doi.org/10.1016/j.jpowsour.2016.06.093>.
- [43] Q. Li, T. Wang, D. Havas, H. Zhang, P. Xu, J. Han, J. Cho, G. Wu, High-performance direct methanol fuel cells with precious-metal-free cathode, *Adv. Sci.* 3 (2016), <https://doi.org/10.1002/adv.201600140>.
- [44] A.H.A. Monteverde Videla, D. Sebastián, N.S. Vasile, L. Osmieri, A.S. Aricò, V. Baglio, S. Specchia, Performance analysis of Fe-N-C catalyst for DMFC cathodes: effect of water saturation in the cathodic catalyst layer, *Int. J. Hydrogen Energy* 41 (2016) 22605–22618, <https://doi.org/10.1016/J.IJHYDENE.2016.06.060>.
- [45] A. Zaffora, F. di Franco, E. Gradino, M. Santamaria, Methanol and proton transport through chitosan-phosphotungstic acid membranes for direct methanol fuel cell, *Int. J. Energy Res.* 44 (2020) 11550–11563, <https://doi.org/10.1002/er.5777>.
- [46] M. Santamaria, C.M. Pecoraro, F. di Franco, F. di Quarto, I. Gatto, A. Saccà, Improvement in the performance of low temperature H<sub>2</sub>-O<sub>2</sub> fuel cell with chitosan-phosphotungstic acid composite membranes, *Int. J. Hydrogen Energy* 41 (2016) 5389–5395.
- [47] J.Y. Park, J.H. Lee, J. Sauk, I. Hyuk Son, The operating mode dependence on electrochemical performance degradation of direct methanol fuel cells, *Int. J. Hydrogen Energy* 33 (2008) 4833–4843, <https://doi.org/10.1016/j.ijhydene.2008.04.060>.
- [48] N. Metzger, X. Li, Technical and economic analysis of fuel cells for forklift applications, *ACS Omega* 7 (2022) 18267–18275, <https://doi.org/10.1021/acsomega.1c07344>.